Asociación Argentina
de Mecánica Computacional

Mecánica Computacional Vol XXX, págs. 3339-3355 (artículo completo)
Oscar Möller, Javier W. Signorelli, Mario A. Storti (Eds.)
Rosario, Argentina, 1-4 Noviembre 2011

MULTI-OBJECTIVE OPTIMIZATION OF THE DYNAMIC OF A BRIDGE PILLAR AND A TRUSS STRUCTURE SUBJECTED TO RANDOM LOAD BY A NEW HYBRIDIZED METHOD

Emmanuel Pagnacco[a], Hafid Zidani[a,b], Rubens Sampaio[c], Rachid Ellaia[b] and Jose E. Souza de Cursi[a]

[a]*LMR, EA 3828, INSA Rouen BP 8, 76801 Saint-Etienne du Rouvray, France, emmanuel.pagnacco@insa-rouen.fr*

[b]*Laboratory of Study and Research for Applied Mathematics, Mohammed V-Agdal University, Engineering Mohammadia School, Rabat, BP. 765, Ibn Sina avenue, Agdal, Morocco, ellaia@emi.ac.ma, hafidzidani@yahoo.fr*

[c]*PUC-Rio, Mechanical Eng. Dept. Rua Marquês de São Vicente, 225 22453-900 Rio de Janeiro RJ. Brazil, rsampaio@puc-rio.br*

Keywords: Representation formula, Nelder-Mead, Multi-objective optimization, Structural dynamics, Mechanical design, Random process, Normal Boundary Intersection approach, Pareto front.

Abstract. In this paper two linear dynamic mechanical problems involving random Gaussian loading are considered for their design through multi-objective optimization problems involving the mean and the standard deviation. It is also presented a new hybridization, called Representation Formula Nelder-Mead, RFNM, for solving global optimization problems. This new hybridization, motivated by the Pincus representation formula hybridized with Nelder-Mead Algorithm, is proposed to solve the two multi-objective optimization problems. The Pincus representation formula gives a good approximation of the global minimum and once one is near the minimum the Nelder-Mead algorithm converges to it rather quickly. The Pincus representation is obtained generating through an uniform distribution a sequence of points and computing an approximation of the minimum; this is done a certain number of times until convergence is achieved.

The first problem is a design of a pillar geometry with respect to a compressive random load process. The second problem is the design of a truss structure with respect to a vertical random load process for several frequency bands. In both problems, the load is characterized by an ergodic, stationary, Gaussian random process. To generate the Pareto front, the Normal Boundary Intersection (NBI) method is used to produce a series of constrained single-objective optimizations. The penalty method is introduced to deal with the new constrains introduced by NBI and in order to put the problems in the framework of the RFNM algorithm used in the single-objective optimizations. The second problem, depending on the frequency band of excitation, can have as Pareto curve a single point, a standard Pareto curve, or a discontinuous Pareto curve. Hence, it is showing through this simple example that difficult situations can occur for designing the mechanical systems when considering their dynamic responses due to random loads, even for this simple situation. But the strategy proposed here have shown its ability to give valuable results, able to help designers to choose for the best compromise between the mean and the standard deviation for this kind of problems.

1 INTRODUCTION

Engineering optimization problems can be very complex and quite difficult to be approximated. They usually are multi-objective and have some stochastic part associated with the parameters or the load. For a multi-objective problem the solution can be viewed as the Pareto front of the problem and an engineering design requires some trade-off among different optimization criteria. In this work, we treat two structural dynamic problems with random loads. Due to the normality of the load process and the linearity of the mechanical problem, the random design problem will be transformed into a deterministic multi-objective optimization problem for the moments of the displacement, hence eliminating the randomness. In this paper only two moments will be considered, the mean and the standard deviation of the temporal displacement. The first problem is somewhat standard and the resulting Pareto curve presents no novelty. The second problem is more interesting and the position of the optimal point for the variance changes with the frequency band chosen for the load. For some frequency bands the Pareto curve is discontinuous, see Fig. 10. To construct the Pareto curve of the multi-objective optimization problem the strategy is first to transform the problem into a sequence of single-objective with constraints problems using the NBI methodology.

The existing literature on Optimization presents intensive research effort to solve some difficult points, which remain still incompletely solved and for which only partial response has been obtained. Among these, we may cite : handling of non-convexity - specially when optimization restrictions are involved, working with incomplete or erroneous evaluation of the functions and restrictions, increasing the number of optimization variables up to those of realistic designs in practical situations, dealing with non-regular (discontinuous or non-differentiable) functions, determining convenient starting points for iterative methods (Floudas et al., 2009; Davidor, 1990).

We observe that the difficulties concerning non-convexity and the determination of starting points are connected: efficient methods for the optimization of regular functions are often deterministic and involve gradients, but depend strongly on the initial point - they can be trapped by local minima if a non convenient initial guess is used. Alternatively, methods based on the exploration of the space of the design variables to search for global solutions, not local ones, usually involve a stochastic aspect - thus, a significant increase in the computational cost - and are less dependent of the initial choice, but improvements in their performance request combination with deterministic methods and may introduce a dependence on the initial choice. Methods designed to find global solutions tend to the use of hybrid procedures, a random search of the space of parameters and, when near the optimum point using methods of quick convergence. They try to benefit from the best of each method - by these reasons, the literature about mixed stochastic-deterministic methods has grown in the last years (Chelouah and Siarry, 2005; Fan and Zahara, 2007; Lee and El-Sharkawi, 2008; Ivorra et al., 2011).

In this paper such a hybrid algorithm is introduced to deal with single-objective optimization problems. By using the penalty method, the problem is put in a framework that allows the use of the modified Pincus algorithm to find a good initialization and then the Nelder-Mead algorithm is used to find a better approximation. This strategy leads to a new algorithm named Representation Formula Nelder-Mead, RFNM. Hence, the RFNM algorithm use a representation formula to provide a convenient initial guess of the solution. It is a hybrid method for solving optimization problems using a coupling of the representation formula proposed by Pincus (1968) and Nelder-Mead algorithm. The representation formula is used first to find the region containing the global solution, and then Nelder-Mead is used to obtain a more accurate approximations.

In this paper, two practical engineering multi-objective optimization problems are presented. One concerning the design of pillar geometry and another the design of a truss structure. In both problems, the load is characterized by an ergodic, stationary, Gaussian random process. To obtain their Pareto front, the NBI methodology is involved with the penalty method, and the resulting subproblems are solved with the help of the RFNM algorithm.

The paper is organized as follows: Section 2 presents the NBI method to generate Pareto front, and the penalty method is recalled in order to deal with constrained subproblems generated by NBI. The representation formula will be mentioned in Section 3, as well as the Nelder-Mead algorithm. Finally, the pillar design and the truss structure design problems are demonstrated in Section 4, followed by some concluding remarks in Section 5.

2 MULTI-OBJECTIVE OPTIMIZATION

2.1 Normal Boundary Intersection method

Multi-objective optimization involves the simultaneous optimization of several incommensurable and often competing objectives. In the absence of any preference information, a non-dominated set of solutions is obtained, instead of a single optimal solution. These optimal solutions are termed as Pareto optimal solutions. Stated in another way, Pareto optimal sets are the set of solutions that cannot be improved in one objective function without deteriorating their performance in at least one of the other objectives (Collette and P., 2003). In general, a Multi-objective problem consists of a vector-valued objective function to be minimized, and of some equality or inequality constraints, i.e.,

$$\begin{cases} \min \;\; \mathbf{F}(\mathbf{x}) = (f_1(\mathbf{x}), ..., f_\ell(\mathbf{x}))^T \\ \text{subject to} \quad d_i(\mathbf{x}) \leq 0 \;,\; i = 1, ..., m, \\ \qquad\qquad\;\; d_j(\mathbf{x}) = 0 \;,\; j = m+1, ..., p, \end{cases} \tag{1}$$

where $\mathbf{x} \in I\!R^n$ is the vector of decision variables, $f_1, ..., f_\ell$ are objective functions, $d_1, .., d_m$ and $d_{m+1}, .., d_p$ are possible sets of inequality and equality constraints, respectively, which represent the process model. This set of constraints defines the feasible space Ω, while the set of all possible values of the objective function constitutes the objective space.

In this work, we are interested with the Normal Boundary Intersection (NBI) method (Das and Dennis, 1998), which could produce an even spread of points on the Pareto front. NBI works by transforming the non-linear Multi-objective optimization problem into a set of non-linear programming subproblem. This recent strategy can be considered as the state of the art regarding deterministic methods. NBI has a number of advantages over other existing methods, including the possibility to obtain an even spread of points in the Pareto set (Das and Dennis, 1998). It uses a geometrically intuitive parameterization to produce a set of points on the Pareto surface, giving an accurate picture of the whole surface. Given any point generated by NBI, it is usually possible to find a set of weights such that this point minimizes a weighted sum of objectives, as described above. Similarly, it is usually possible to define a goal programming problem for which the NBI point is a solution. NBI can also handle problems where the Pareto surface is discontinuous or non-smooth, unlike homotopy techniques. Unfortunately, a point generated by NBI may not be a Pareto point if the boundary of the attained set in the objective space containing the Pareto points is non-convex or 'folded' (which happens rarely in problems arising from actual applications). NBI requires the individual minimizers of the individual functions at the outset, which can also be viewed as a drawback. The formulation (1), however, must be interpreted as an alternative way. Instead of one objective function, we have ℓ objective functions which we want to reduce subject to the constraints. Since some of the objective

functions may conflict with others, one has to find an appropriate compromise depending on priorities of the user. The ideal situation would be the existence of a vector $\mathbf{x}^*$ with

$$(f_1(\mathbf{x}^*), ..., f_\ell(\mathbf{x}^*)) = (f_1^*, ..., f_\ell^*)$$

where each $f_i^*, \;\; i = 1, ..., \ell$, the individual minima of the corresponding scalar problem

$$\begin{cases} \min \;\; f_i(\mathbf{x}) \\ \text{subject to } \; \mathbf{x} \in \Omega \end{cases} \tag{2}$$

for $i = 1, ..., \ell$. But of course this is an ideal situation and normally the individual minimum f_i^* will be attained at different points. NBI essentially works by solving sequentially a set of single nonlinear problems (NBI subproblems), which are defined as:

$$\begin{cases} \max\limits_{\mathbf{x},s} \;\; s \\ \text{subject to } \;\; \mathbf{\Phi}.\mathbf{w} + s.\hat{\mathbf{n}} = \mathbf{F}\left(\mathbf{x}\right) - \mathbf{f}^*, \\ \qquad\qquad \mathbf{x} \in \Omega \end{cases} \tag{3}$$

$\mathbf{\Phi}$ be the $\ell \times \ell$ pay-off matrix in which i^{th} column is $\mathbf{F}(\mathbf{x}_i^*) - \mathbf{f}^*$, where $\mathbf{f}^*$ is the vector of the individual minima (i.e., the utopia point or shadow minimum) and $\mathbf{x}_i^*$ is the minimizer of objective f_i (i.e., minimizers of problem (2)). $\mathbf{w}$ is a vector of weights such that $\sum\limits_{i=1}^{\ell} w_i = 1$, $w_i \geq 0$, and $\hat{\mathbf{n}}$ is the quasi-normal direction which has negative components, i.e. it points towards the origin. Φw defines a point on the so-called Convex Hull of Individual Minima (CHIM). Then the set of points in $\mathbb{R}^n$ that are convex combinations of $f_i^* - \mathbf{f}^*$, i.e, $\mathbf{\Phi w}$, is referred to as the CHIM.

Now let us illustrate algebraically how any such boundary point can be found by solving an optimization problem. Given barycentric coordinates $\mathbf{w}$, $\mathbf{\Phi w}$ represents a point in the CHIM. Let $\hat{\mathbf{n}}$ denote the unit normal to the CHIM simplex pointing towards the origin, then $\mathbf{\Phi}.\mathbf{w} + s.\hat{\mathbf{n}}$, $s \in \mathbb{R}$ represents the set of points on the normal. Thus, in traditional NBI, $\hat{\mathbf{n}}$ is chosen to be $-\mathbf{\Phi}.\mathbf{e}$ where $\mathbf{e}$ is the column vector of all ones. The intersection between the normal to the CHIM from the point and the boundary of the objective space $\mathcal{F}$ closest to the origin is expected to be Pareto-optimal. This is done for various $\mathbf{w}$, so that an equally distributed set of them produces an equally distributed set of non-dominated points, which is an useful feature for the decision-making process. If the Pareto set is convex and the individual minima of the objective are the global ones, the solution to this problem is Pareto optimal.

The subproblem (3) shall be referred as the NBI subproblem and written as NBI_w, since $\mathbf{w}$ is the characterizing parameter of the subproblem. The solution of these subproblems will be referred to as NBI points. The idea is to solve NBI_w for various $\mathbf{w}$ and find several points on the boundary of $\mathcal{F}$, effectively constructing a point-wise approximation of the efficient frontier. As indicated earlier, all NBI points are not Pareto optimal points. In bi-objective problems, for every Pareto optimal point, there exists a corresponding NBI subproblem of which it is solution.

2.2 Penalty method

One common approach to deal with the constrained optimization problems such as the one given by the problem (3) is to introduce a penalty term into the objective function to penalize constraint violations (Luenberger, 1973; Avriel, 1976). The introduction of the penalty term enables us to transform a constrained optimization problem into an unconstrained one, such as:

$$\text{minimize } F_{r,p} = s + r\varphi_p\left(\mathbf{x}\right)$$

with penalty

$$\varphi_p(\mathbf{x}) = \mid \mathbf{\Phi}.\mathbf{w} + s.\hat{\mathbf{n}} - \mathbf{F}\left(\mathbf{x}\right) + \mathbf{f}^* \mid^p$$

where $r > 0$ is a positive penalty parameter and p the penalty exponent. If $p = 1$ it can be proved that the penalty function is exact, i.e. for some sufficiently large value of $r > 0$ any global minimum is a global minimum. However, the exact penalty function is not always differentiable at all points. For that reason the values $p > 1$, which guarantee differentiability, are also used. In this case the solutions under mild conditions converge to a global minimum when $r \longrightarrow \infty$, see ref. (Luenberger, 1973; Avriel, 1976). If r is too small, an infeasible solution may not be penalized enough. If r is too large, a feasible solution is very likely to be found, but could be of very poor quality. A large r discourages the exploration of infeasible regions even in the early stages of evolution. This is particularly inefficient for problems where feasible regions in the whole search space are disjoint. In this case it is difficult to move from one feasible region to another unless they are very close to each other. Reasonable exploration of infeasible regions may act as bridges connecting two or more different feasible regions. The critical issue here is how much exploration of infeasible regions (i.e., how large r is) should be considered as reasonable.

3 RFNM ALGORITHM

In order to find the Pareto front of optimization problems, we propose in this work to solved the set of nonlinear programming subproblem obtained from the NBI method by means of a hybrid Nelder-Mead simplex search with integral representation formula.

Nelder-Mead (Nelder and Mead, 1965) algorithm is well known for its popularity and ease of use and does not need the derivation of the function under exploration. In this study, one interesting feature of this algorithm is its ability to handle difficult to minimize objective functions such that the one obtained here by using the penalty method. However, it is a local approach, and is very sensitive to the choice of initial points and does not ensure to attain the global optimum. Hence, It would be interesting to hybridize it with the formula method of Pincus (1970) to generate the initial point. This hybrid method is proposed here and called RFNM. It is an improvement of the Nelder-Mead algorithm by using first the representation formula to find the region containing the global solution, based on the generating of finite samples of the random variables involved in the expression and an approximation of the limits.

3.1 About the Representation Formula of Pincus

Let $\mathcal{S}$ denote a closed bounded regular domain of the n-dimensional Euclidean space $\mathbb{R}^n$, and let f be a continuous scalar function defined on $\mathcal{S}$ and taking its values on $\mathbb{R}$. A constrained optimization problem can be formulated, in general, as follows :

$$x^* = \arg \min_{x \in \mathcal{S}} f(x) \tag{4}$$

In the literature, representation formulas have been introduced in order to characterize explicitly solutions of the problem 4. In general, these representations assume that $\mathcal{S}$ contains a single

optimal point x^* (but many local minima may exist on $\mathcal{S}$). For instance, Pincus (1968, 1970) has proposed the representation formula :

$$x^* = \lim_{\varrho \to +\infty} \frac{\int_S x\, e^{-\varrho f(x)} dx}{\int_S e^{-\varrho f(x)} dx}. \tag{5}$$

An extension to multiple minima may be found in Charnes and Wolfe (1989) and an approach based on the boundedness of a sequence of integrals has been proposed by Falk (1973). More recently, the original representation proposed by Pincus has been reformulated by Souza de Cursi (2007) as follows: let X be a random variable taking its values on $\mathcal{S}$ and $g : I\!R^2 \longrightarrow I\!R$ be a function. If these elements are conveniently chosen, then :

$$x^* = \lim_{\lambda \to +\infty} \frac{\mathrm{E}\left(X\, g\left(\lambda, f(X)\right)\right)}{\mathrm{E}\left(g\left(\lambda, f(X)\right)\right)} \tag{6}$$

where $\mathrm{E}\left(\bullet\right)$ denote the expected operator. The formulation of Pincus corresponds to $g\left(\lambda, s\right) = e^{-\lambda s}$, which is a convenient choice. The general properties of X and g are detailed, for instance, in Bez et al. (2004); Souza de Cursi et al. (2008). X is a convenient random variable (see, for instance, (Souza de Cursi, 2007)) and these conditions are fulfilled, for instance, when X is uniformly distributed or Gaussian.

This equation may be interpreted as a weighted mean of the points $x \in \mathcal{S}$, where the weight decreases when $f(x)$ increases. The term $g\left(\lambda, f(x)\right)$ in the representation formula vanishes for points having values higher than $f(x^*)$ when $\lambda \to +\infty$. Although this mathematical result seems to be very attracting, it is very difficult to implement codes using this representation. In this paper we suggest to use a numerical approximation based of finite samples of the random variables involved in the expression and an approximation of the limit.

A numerical implementation can be performed by taking a large fixed value of λ in order to represent the limit $\lambda \to +\infty$. In order to prevent an overflow, λ should be increased gradually up to the desired value and it may be convenient to use positive functions f (for instance, by adding a constant to the original f). A finite sample of X is generated, according to a given probability - this consists simply in generating N admissible points $(x_1, x_2, ..., x_N) \in \mathcal{S}$ - and estimations of the means are used to approximate the exact means, what leads to :

$$x^* \simeq x_c^* = \frac{\sum_{i=1}^{N} x_i \;\; g\left(\lambda, f(x_i)\right)}{\sum_{i=1}^{N} g\left(\lambda, f(x_i)\right)} \tag{7}$$

3.2 Nelder-Mead Algorithm

The Nelder-Mead algorithm (NM), or downhill simplex algorithm, has been proposed by Nelder and Mead (1965). It is a simple direct search technique that has been widely used in unconstrained optimization problems. One of the reasons for its popularity is that this method is easy to use and does not need any derivative information. This is a very important feature in cases where gradient information is not available. However, we should be very careful when using this method since it is very sensitive to the choice of initial points and not guaranteed to obtain the global optimum. This algorithm makes use of four scalar parameters: coefficient of reflection (ϑ), expansion (χ), contraction (γ), and shrinkage (δ). According to the original Nelder-Mead paper (Nelder and Mead, 1965), these parameters should satisfy :

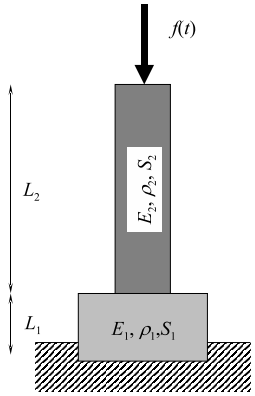

Figure 1: Sketch and dimensions of the pillar

$$\vartheta > 0, \quad \chi > 1, \quad \chi > \vartheta, \quad 0 < \gamma < 1, \quad \text{and} \quad 0 < \delta < 1.$$

In the standard Nelder-Mead algorithm, this coefficient are chosen as follows :

$$\vartheta = 1, \quad \chi = 2, \quad \gamma = \frac{1}{2}, \quad \text{and} \quad \delta = \frac{1}{2}. \tag{8}$$

This method starts with a simplex of $n+1$ vertices, each of which is a point in $\mathbb{R}^n$. These vertices are labeled $x_1, x_2, \ldots, x_{n+1}$, such that $f(x_1) \leq f(x_2) \leq \ldots \leq f(x_{n+1})$. Since f is to be minimized, x_1 is the best point and x_{n+1} is the worst point. At each step in the iteration, the current worst point x_{n+1} is discarded, and another point is accepted into the simplex. This process continues until convergence is achieved.

4 TWO DESIGN PROBLEMS

4.1 Pillar Design Problem

The first problem considered is a design of a little bridge pillar having length L and made from two parts (see Figure 1). The first part is made out of concrete, and the second is made of steel. We denote the Young's modulus and density by E_1 and ρ_1 for the concrete and E_2 and ρ_2 for the steel. The concrete pillar geometry have a length L_1 with a constant cross-section area S_1 while the steel pillar have a constant area S_2 with a length L_2 such that $L = L_1 + L_2$. For the numerical application, we have chosen $E_1 = 3.6 \times 10^{10}$ Pa, $E_2 = 2.1 \times 10^{11}$ Pa, $\rho_1 = 2500$ kg/m^3, $\rho_2 = 7800$ kg/m^3 and $L = 15$ m, while other quantities have to be found by the optimization procedure. However, S_1 and S_2 have to be greater than some prescribed values to ensure that the pillar is not irreversibly deformed and the material remains in the elastic range, while L_1 has to be greater or equal to 1 m in order to ensure the feasibility of the concrete pillar foundation.

In this study, only the axial movement of the pillar is of interest, assuming the bottom at $y = 0$ is fixed while the tip at $y = L$ is subjected to a mean plus a fluctuating or a moving load. From the linear continuum mechanic, when the damping, the gravity load and the transverse effects are not considered, equations to be verified in the pillar are (Géradin and Rixen, 1996):

$$\begin{cases} -E_1 \frac{\partial^2 u}{\partial y^2} = \omega^2 \rho_1 u\,(y,\omega) & \text{for } 0 \leq y \leq L_1 \\ -E_2 \frac{\partial^2 u}{\partial y^2} = \omega^2 \rho_2 u\,(y,\omega) & \text{for } L_1 \leq y \leq L \end{cases} \tag{9}$$

with the boundary and compatibility conditions:

$$\begin{cases} u\left(y,\omega\right)=0 & \text{for } y=0 \\ -E_2S_2\frac{\partial u}{\partial y}=p\left(\omega\right) & \text{for } y=L \\ -E_1S_1\frac{\partial u}{\partial y}=E_2S_2\frac{\partial u}{\partial y} & \text{for } y=L_1 \end{cases} \tag{10}$$

where $u\left(y,\omega\right)$ and $p\left(\omega\right)$ denotes respectively the deterministic longitudinal displacement field and the tip load in the frequency domain, ω being the circular frequency. Moreover, the field u has to be continuous everywhere in the pillar, thus also at the interface between the two parts (which constitutes a second compatibility condition). Introducing the wave speeds $c_1=\sqrt{\frac{E_1}{\rho_1}}$ and $c_2=\sqrt{\frac{E_2}{\rho_2}}$, the solution is sought in the form

$$u\left(y,\omega\right)=\begin{cases} C_1\cos\left(\frac{\omega y}{c_1}\right)+D_1\sin\left(\frac{\omega y}{c_1}\right) & \text{for} \quad 0\leq y\leq L_1 \\ C_2\cos\left(\frac{\omega y}{c_2}\right)+D_2\sin\left(\frac{\omega y}{c_2}\right) & \text{for} \quad L_1\leq y\leq L \end{cases}$$

where C_i and D_i are constants to be determined from the four boundary and compatibility conditions. However, only the displacement u at the extremity $y=L$ of the pillar is of interest for the design. Introducing variables $\alpha_i=\omega\frac{L_i}{c_i}$ and $\beta_i=\frac{E_iS_i}{L_i}\alpha_i$ for $i=\{1,2\}$, it is found after some manipulations that:

$$u\left(y,\omega\right)=\begin{cases} \frac{\sin\left(\alpha_1\frac{x}{L_1}\right)}{\sin(\alpha_1)}u\left(y=L_1,\omega\right) & \text{for} \quad 0\leq y\leq L_1 \\ \frac{\sin\left(\alpha_2\frac{L-x}{L-L_1}\right)}{\sin(\alpha_2)}u\left(y=L_1,\omega\right)+\frac{\sin\left(\alpha_2\frac{L_1-x}{L_1-L}\right)}{\sin(\alpha_2)}u\left(y=L,\omega\right) & \text{for} \quad L_1\leq y\leq L \end{cases}$$

with:

$$u\left(y=L_1,\omega\right)=\left(\frac{\beta_1}{\tan\left(\alpha_1\right)\tan\left(\alpha_2\right)}-\beta_2\right)^{-1}\frac{p\left(\omega\right)}{\sin\left(\alpha_2\right)}$$

and

$$u\left(\omega,y=L\right)=h\left(\omega\right)\times p\left(\omega\right)$$

where $h\left(\omega\right)$ is the frequency response function of the pillar tip at $x=L$ and is such that:

$$h\left(\omega\right)=\frac{1}{\beta_2}\left(\frac{\beta_1}{\tan\left(\alpha_1\right)\tan\left(\alpha_2\right)}-\beta_2\right)^{-1}\left(\frac{\beta_1}{\tan\left(\alpha_1\right)}+\frac{\beta_2}{\tan\left(\alpha_2\right)}\right)$$

However, since real structures are damped, we added some light hysterectic damping in this model by replacing real speed sound constants c_i by complex speed sounds $\tilde{c}_i$ such that $\tilde{c}_i=c_i\left(1+j\eta_i\right)$ with the damping factors η_i having the arbitrary value $\eta_i=0.07$.

In this problem, we are interested to design the pillar geometry in respect to a compressive random load process $P\left(t\right)$, where t denotes the time. This load is supposed to be a Gaussian ergodic and stationary random process (Lin, 1967; Wijker, 2009). Thus, it could be describe by its mean $\mu_{\mathrm{p}}=\mathrm{E}\left(P\left(t\right)\right)$ and its covariance function $\Sigma_{\mathrm{pp}}\left(\tau\right)=\mathrm{E}\left(\left(P\left(t\right)-\mu_{\mathrm{p}}\right)\left(P\left(t+\tau\right)-\mu_{\mathrm{p}}\right)\right)$ or its power spectral density (PSD) function $\Phi_{\mathrm{pp}}\left(\omega\right)=\int_{-\infty}^{+\infty}\Sigma_{\mathrm{pp}}\left(\tau\right)\mathrm{e}^{-j\omega\tau}\mathrm{d}\tau$. Hence, its probability density function is given by:

$$\phi(p)=\frac{1}{\sqrt{2\pi\sigma_{\mathrm{p}}^2}}\exp\left(-\frac{\left(p-\mu_{\mathrm{p}}\right)^2}{2\sigma_{\mathrm{p}}^2}\right)$$

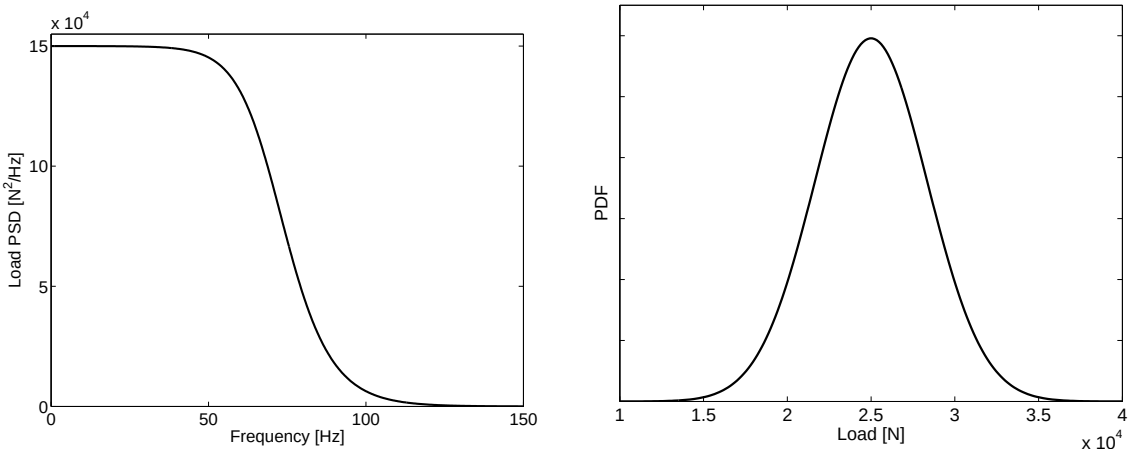

Figure 2: PSD and PDF of the load applied to the pillar

where $\sigma_{\mathrm{p}}^2 = \Sigma_{\mathrm{pp}}(0) = \frac{1}{2\pi}\int_{-\infty}^{+\infty} \Phi_{\mathrm{pp}}(\omega)\,\mathrm{d}\omega$ is named the zero-th spectral moment or the variance load. For the present example, the load of interest has a mean $\mu_{\mathrm{p}} = 25,000$ N due to the roadway and a PSD which can be represented by a generalized logistic function in order to modeled experimental data (for instance, reference (Gillespie, 1992) shows some of these data):

$$\Phi_{\mathrm{pp}}(\omega) = \frac{\kappa}{\left(1 + \kappa \exp\left(-\zeta\left(\omega/2\pi - \tau\right)\right)\right)^{1/\nu}}$$

with $\kappa = 150,000$, $\zeta = -0.15$, $\tau = 150$ and $\nu = 1.4$. This PSD is plotted on Figure 2.

Since we consider a linear structure, the random response is also Gaussian for a Gaussian load. It is thus sufficient to characterize this response by its mean μ_{u} and variance σ_{u}^2. We have

$$\mu_{\mathrm{u}} = h(\omega = 0) \times \mu_{\mathrm{p}}$$

or

$$\mu_{\mathrm{u}} = \left(\frac{L_1}{E_1 S_1} + \frac{L_2}{E_2 S_2}\right) \times \mu_{\mathrm{p}}$$

and $\sigma_{\mathrm{u}}^2 = \frac{1}{2\pi}\int_{-\infty}^{+\infty} \Phi_{\mathrm{uu}}(\omega)\,\mathrm{d}\omega$ with:

$$\Phi_{\mathrm{uu}}(\omega) = h(\omega)\,\Phi_{\mathrm{pp}}(\omega)\,\overline{h}(\omega)$$

where $\overline{\bullet}$ stands for the complex conjugate operator.

For the formulation of the optimization problem, the total mass of the pillar given by

$$m = \rho_1 S_1 L_1 + \rho_2 S_2 L_2$$

is fixed at a value $\hat{m}$. This limitation about the mass is due to the allowable bearing capacity which is the capacity of the soil to support the loads applied to the ground and is given by an experimental geotechnical study. While this experimental study is not achieved, it would be interesting to find the optimal design solution for several arbitrary value $\hat{m}$. In addition, there is a lower limitation for the two areas S_1 and S_2 to ensure the pillar will rest in the elastic range. Such limitations have to be evaluated from the allowable stress which is issue of compressive yield strength of the considered materials and when considering a safety margin. In this study, this is ensure if both areas are greater than 0.0002 m^2.

Engineering with a classical one goal optimization strategy consist generally in finding parameters which minimize the mean displacement plus a given amount of the standard deviation (three times the standard deviation is usually chosen for a Gaussian random variable). In this study, we examine instead the Pareto front of a two-objective optimization, the first being the mean and the second being the standard deviation. This enable to choose the best design from additional engineering constraints, such as a best compromise between the mean stress which has to be supported by materials and a prescribe level of vibration, knowing it is an acceptable level of human comfort.

Finally, the optimization problem is formulated in the following form:

$$\begin{cases} \min \mathbf{F}(S_1, S_2, L_1) & = & (\mu_{\mathrm{u}}(S_1, S_2, L_1), \sigma_{\mathrm{u}}(S_1, S_2, L_1))^T \\ \text{subject to} & & S_i \leq 0.0002,\ i = 1, 2, \\ & & 1 \leq L_1 \leq 15, \\ & & \rho_1 S_1 L_1 + \rho_2 S_2 (L - L_1) = \hat{m} \end{cases}$$

where $\hat{m}$ is a parameter to be chosen.

For all optimization with fixed mass $\hat{m}$, limitations on area are not active since optima are found for $L_1 = 1$ m, meaning that the pillar have to be made with steel is the best one (except for the imposed concrete foundation). This have a good physical sense when considering the density of each material and the limitation imposed for the mass. However, the best mean displacement and the best standard deviation are obtained for different values of design variables S_1 and S_2. For instance, when the total mass is fixed at $\hat{m} = 1,000$ kg, the best mean displacement, which has a value of 0.219 mm, is achieved for $S_1 = 0.036$ m^2 and $S_2 = 0.0083$ m^2, while the best standard deviation displacement, which has a value of 0.0513 mm, is achieved for $S_1 = 0.056$ m^2 and $S_2 = 0.0079$ m^2. When the total mass is fixed at $\hat{m} = 1,500$ kg, the best mean displacement, which has a value of 0.146 mm, is achieved for $S_1 = 0.053$ m^2 and $S_2 = 0.0125$ m^2, while the best standard deviation displacement, which has a value of 0.0342 mm, is achieved for $S_1 = 0.082$ m^2 and $S_2 = 0.0118$ m^2. As it is expected, all the objectives have best values when considering a higher total mass. The PDF of the tip displacement for these two mass cases are presented on the Figure 3. Two curves are plotted for each situation, one (for the best standard deviation) with a thick line and the other (for the best mean) with a dashed line to show both optima.

Finally, optimization results are easily found from the NBI methodology with the RFNM algorithm and the Pareto front obtains for the two mass cases are presented on the Figure 4. These graphics shows that the Pareto front has a standard continuous and convex shape, which help to choose for the best compromise between the mean and the standard deviation of the tip of the pillar.

4.2 Truss structure design

As a second application, we consider a two-bar truss (see Figure 5). Both bars are made of steel. We denote E and ρ the deterministic material properties (Young's modulus and density) of the steel. The horizontal bar have a length L_1 with a constant area S_1 while the other bar have a constant area S_2 with a length L_2 such that $L_2 = \frac{L_1}{\cos(\theta)}$ where $\theta = \frac{\pi}{4}$ rd. is the angle between the two bars. For the numerical application, we have chosen $E = 2.1 \times 10^{11}$ Pa, $\rho = 7800$ m^3 and $L_1 = 1$ m, while other quantities have to be found by the optimization procedure. However, arbitrary bounds for the areas are defined such that $2.2 < S_1 < 20$ and $5 < S_2 < 10$ if there are expressed in mm^2.

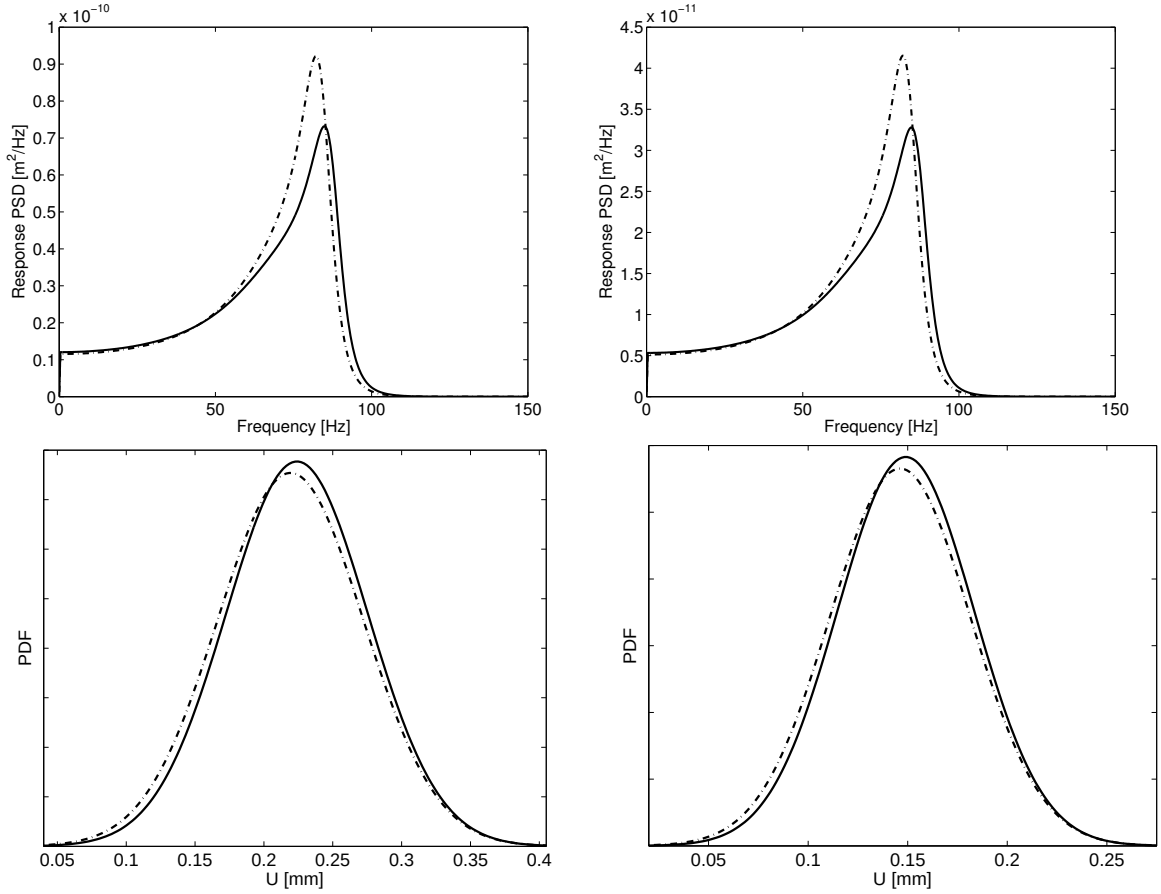

Figure 3: Tip response displacement PSD and PDF for a 1,000 (left) and a 1,500 kg (right) pillars

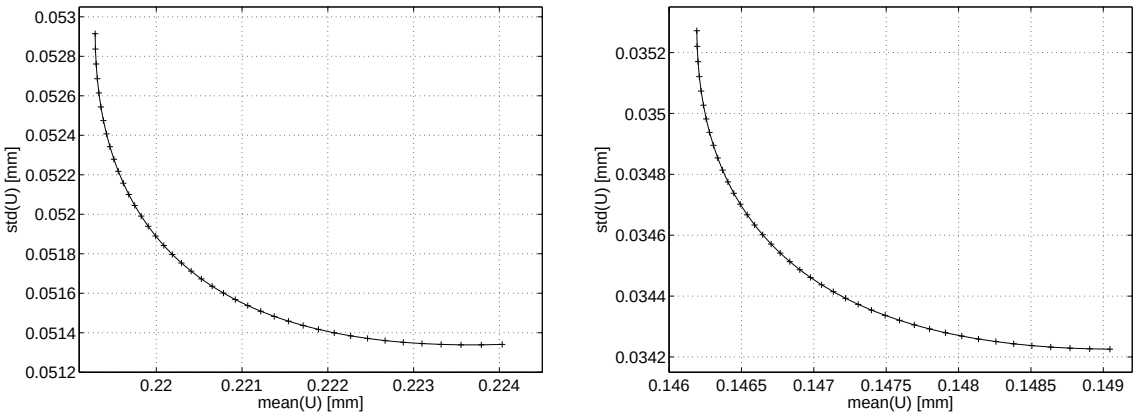

Figure 4: Pareto for a 1,000 (left) and a 1,500 kg (right) pillars; μ_U is denoted mean(U) and σ_U is std(U)

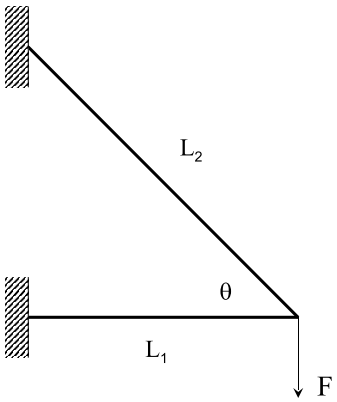

Figure 5: Sketch and dimensions of the two-bar truss

In this study, left ends of the two bars are clamped while the right end is subjected to a mean plus a fluctuating load. First-order finite elements are used to model the bar. From the assembly of the two finite element and when boundary conditions are taken into account, we obtain the discrete global equilibrium (Géradin and Rixen, 1996):

$$\left(\mathbf{K} - \omega^2 \mathbf{M}\right) \mathbf{u}\left(\omega\right) = \mathbf{p}\left(\omega\right) \tag{11}$$

having two degrees of freedoms $\mathbf{u} = \begin{bmatrix} u \\ v \end{bmatrix}$ with u and v are the horizontal and vertical displacement (respectively) and with the stiffness matrix $\mathbf{K}$ and mass matrix $\mathbf{M}$ such that:

$$\mathbf{K} = \begin{bmatrix} k_1 + k_2 \cos^2\left(\theta\right) & k_2 \cos\left(\theta\right) \sin\left(\theta\right) \\ k_2 \cos\left(\theta\right) \sin\left(\theta\right) & k_2 \sin^2\left(\theta\right) \end{bmatrix} \qquad \text{and} \qquad \mathbf{M} = m \begin{bmatrix} 1 & 0 \\ 0 & 1 \end{bmatrix}$$

where $k_1 = ES_1L_1$ and $k_2 = ES_2L_2$ and $m = \frac{\rho}{3}\left(S_1L_1 + S_2L_2\right)$. In this equation, the load vector acts only in the vertical direction. It is such that $\mathbf{p}\left(\omega\right) = \begin{bmatrix} 0 \\ p\left(\omega\right) \end{bmatrix}$. The system (11) can be inverted to leads to the vertical displacement, which is the displacement of interest:

$$v\left(\omega\right) = h\left(\omega\right) \times p\left(\omega\right)$$

where $h\left(\omega\right)$ is the frequency response function of truss and is such that:

$$h\left(\omega\right) = \left(\frac{k_2\left(k_1 - \omega^2 m\right) \sin^2\left(\theta\right)}{k_1 - \omega^2 m + k_2 \cos^2\left(\theta\right)} - \omega^2 m \right)^{-1}$$

Notice that this response function can have both poles and zeros for some values of the design parameters, leading to resonant and anti-resonant frequencies.

In this second problem, we are interested to design the truss in respect to a vertical load process $P\left(t\right)$ having a 200 Hz frequency band. This load is supposed to be a Gaussian, stationary random process, and ergodic. Thus, it could be describe by its mean $\mu_p = 10,000$ N and its PSD which can be modeled by a constant function over the limited range of frequencies:

$$\Phi_{pp}\left(f\right) = \begin{cases} 2000 & \text{if } f_1 \leq f \leq f_2 \\ 0 & \text{if not} \end{cases}$$

Three frequency bands are investigated here: $(f_1, f_2) = (0, 200)$, $(100, 300)$ or $(600, 800)$ Hz. The last one, i.e. $(600, 800)$ Hz, can include an anti-resonant frequency for some values of the design parameters.

Since we consider a linear structure, the random response is also Gaussian for a Gaussian load. It is thus sufficient to characterize this response by its mean μ_{v} and standard deviation σ_{v}. We have

$$\mu_{\mathrm{v}} = h\left(\omega = 0\right) \times \mu_{\mathrm{p}}$$

or

$$\mu_{\mathrm{v}} = \left(\frac{1}{k_1 \tan^2\left(\theta\right)} + \frac{1}{k_2 \sin^2\left(\theta\right)} \right) \times \mu_{\mathrm{p}}$$

and $\sigma_{\mathrm{v}}^2 = \frac{1}{2\pi} \int_{-\infty}^{+\infty} \Phi_{\mathrm{vv}}\left(\omega\right) \mathrm{d}\omega$ with:

$$\Phi_{\mathrm{vv}}\left(\omega\right) = h\left(\omega\right) \Phi_{\mathrm{pp}}\left(\omega\right) \overline{h}\left(\omega\right)$$

In this problem, we are again interested to find the Pareto front of a two-objective optimization, namely the mean and the standard deviation. The optimization problem is thus formulated in the following form:

$$\left\{ \begin{array}{lcl} \min \ \mathbf{F}\left(S_1, S_2\right) & = & \left(\mu_{\mathrm{v}}\left(S_1, S_2\right), \sigma_{\mathrm{v}}\left(S_1, S_2\right)\right)^T \\ \text{subject to} & & 22 \leq S_1 \leq 200 \\ & & 50 \leq S_2 \leq 100 \end{array} \right.$$

Notice that for this problem μ_{v} is a convex function whereas σ_{v} is not. See Figures 7, 8, 9 for a contour plot of these two functions in the frequency bands $0 - 200$, $100 - 300$, and $600 - 800$ Hz. The optimum of the mean, in all three cases, is located at the boundaries for the design variables, for their maximum values; it is the point a in Figures 7, 8, 9. From the mechanical equations, it is trivial since one can observe that the mean displacement is related to the static deflexion mode. Hence it is a highly logical design, since using more material leads to a higher truss stiffness, reducing consequently its global displacement. On the other hand, the variance function has two minimum, located at the boundary of the domain. One of these minimum, point a, being a local minimum for the design $(S_1, S_2) = (200, 100)$, the other one being a global minimum, point c, for the design $(S_1, S_2) = (22, 100)$. Moreover, notice that this global optimum is located in a deep valley. The physical reason of such a behavior comes from the presence -or not- of the anti-resonant frequency in the range of interested (excited) frequencies. In order to better understand this explanation, the complete PSD over a large frequency range is presented on the Figure 6, showing the location of the resonant and anti-resonant frequencies for the two optimal design.

In the first step, to obtain the utopia point, or, equivalently, the two extremal points of the Pareto Front, the RFNM algorithm is used. Initial guess points for the NM algorithm are evaluated with the Pincus representation formula presented in this work from a uniform distribution having a one hundred sample size. Next, in the second step, other Pareto front point of this problem are given by the NBI method using $\hat{\mathbf{n}} = -\mathbf{\Phi}.\mathbf{e}$ with $\mathbf{e} = (1, 1)^T$ (by taking the proposal of Das and Dennis (1998)) and a penalty parameter chosen to be $r = 10^5$. Each NBI points are then given by the RFNM algorithm with the same parameters as in the first step. Depending on the stating point given by the Pincus representation formula, the Nelder-Mead algorithm takes approximately 150 to 300 function evaluations to converge with relative stopping criteria fixed at the value 10^{-3} for the improvement in both the performance function and the design parameters.

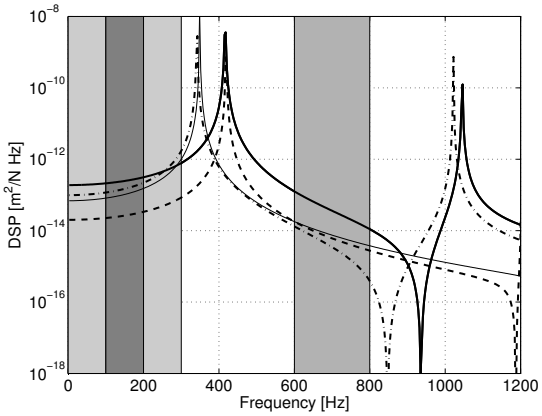

Figure 6: PSD of the two-bar truss for four extremum designs; continuous thick line: $S_1 = 22$ mm^2 and $S_2 = 50$ mm^2 ; dashed line: $S_1 = 22$ mm^2 and $S_2 = 100$ mm^2 ; continuous thin line: $S_1 = 200$ mm^2 and $S_2 = 50$ mm^2 ; dotted line: $S_1 = 200$ mm^2 and $S_2 = 100$ mm^2

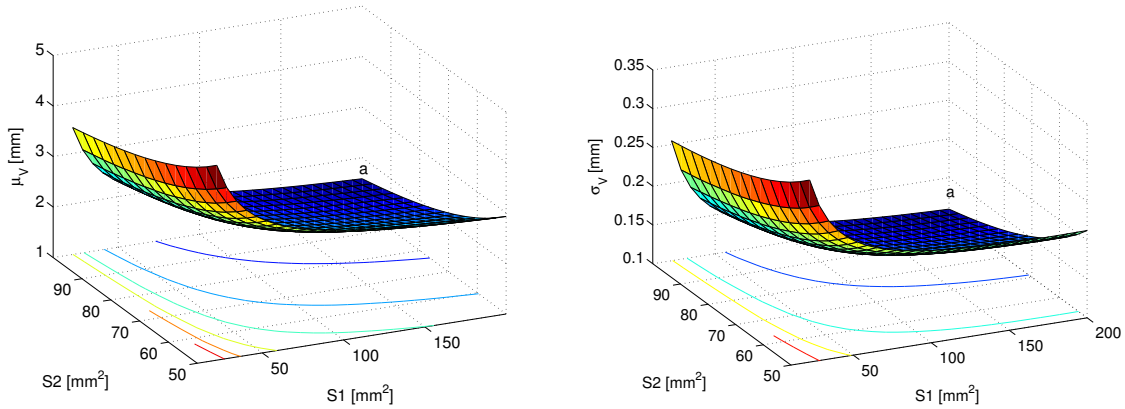

Figure 7: Response surfaces of the two-bar truss for the mean (left) and the standard deviation (right) over the frequency band $(0, 200)$ Hz

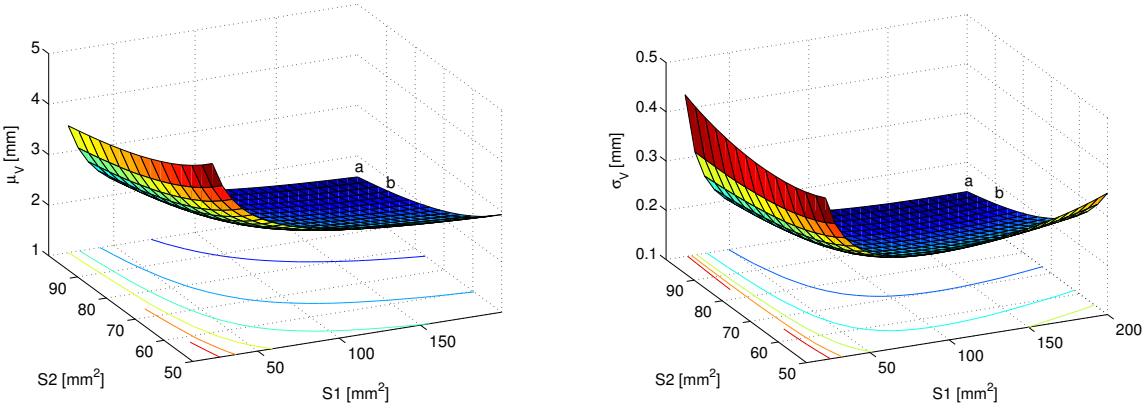

Figure 8: Response surfaces of the two-bar truss for the mean (left) and the standard deviation (right) over the frequency band $(100, 300)$ Hz

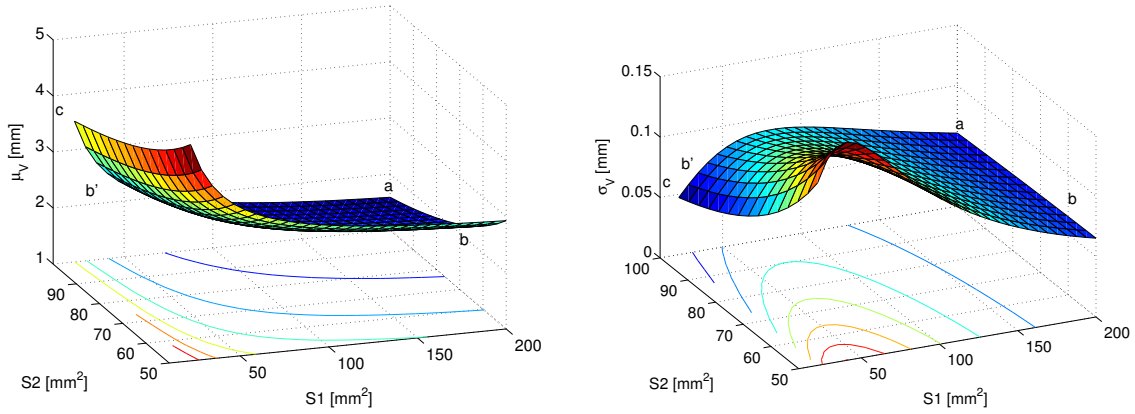

Figure 9: Response surfaces of the two-bar truss for the mean (left) and the standard deviation (right) over the frequency band $(600, 800)$ Hz

The Pareto front of this two-bar truss for the frequency band $(0, 200)$ Hz is not presented on some Figure, since it is reduces to only one, single point, indicating that both the minimum mean and the minimum variance are achieve with same values for the parameters design, namely the one with the maximum values for the both parameters. The Pareto front of this two-bar truss for the frequency band $(100, 300)$ and $(600, 800)$ Hz are presented on the Figure 10. For the frequency band $(100, 300)$ Hz, the Pareto front has a standard continuous and convex shape, since both function to be minimized has only one minima, locating at different design parameters values for each one.

For the frequency band $(600, 800)$ Hz, it can be observing that the Pareto front is discontinuous. Starting from the leftmost point, $a = (1.58, 0.605)$, that is a Pareto point, the next Pareto point in the curve is the one immediately below the first Pareto point. The intervening points are not Pareto points. From a, that corresponds to $(S_1, S_2) = (200, 100)$, the next point in Figure 10, $b = (2.73, 0.65)$ corresponds to $(S_1, S_2) = (200, 54)$ and the curve is for $S_1 = 200$. The discontinuity occurs and the point $b' = b$, that now corresponds to $(S_1, S_2) = (34.4, 100)$ and begins another curve just to point $c = (3.51, 0.472)$ that corresponds to $(S_1, S_2) = (22, 100)$ and this curve has $S_2 = 100$. As one sees, the discontinuity in Pareto's curve corresponds to a discontinuity in the design variables. This is clearly seen on the Figure 9.

Results presented on the Figure 10-down-left shows also that the choice for $\hat{\mathbf{n}}$ is not adequate for this problem and failed to give the even spread set of distributed points. In fact, Pareto front points can be better distributed being careful to choose adequately the normal ($\mathbf{e} = (1, 0.3)^T$ for instance, in order to produce the Pareto front presented on Figure 10-down-right).

These Pareto's curves helps to choose the best compromise between the mean and the standard deviation of the truss vertical displacement.

5 CONCLUSIONS

Optimization of dynamical linear structures with Gaussian loading is investigated here through two simple examples of mechanical design. Dimensioning these structures is generally a multi-objective task in order to achieve a robust design. Moreover, it appears here for the second example, which involves the minimization of the standard deviation of a simple two bars truss, that the function is not convex with multiple minima for the frequency band $(600, 800)$ Hz, since it involves an anti-resonance frequency for some values of the design parameters.

Multi-objective problems are treated via a Pareto front. In order to construct this front, the

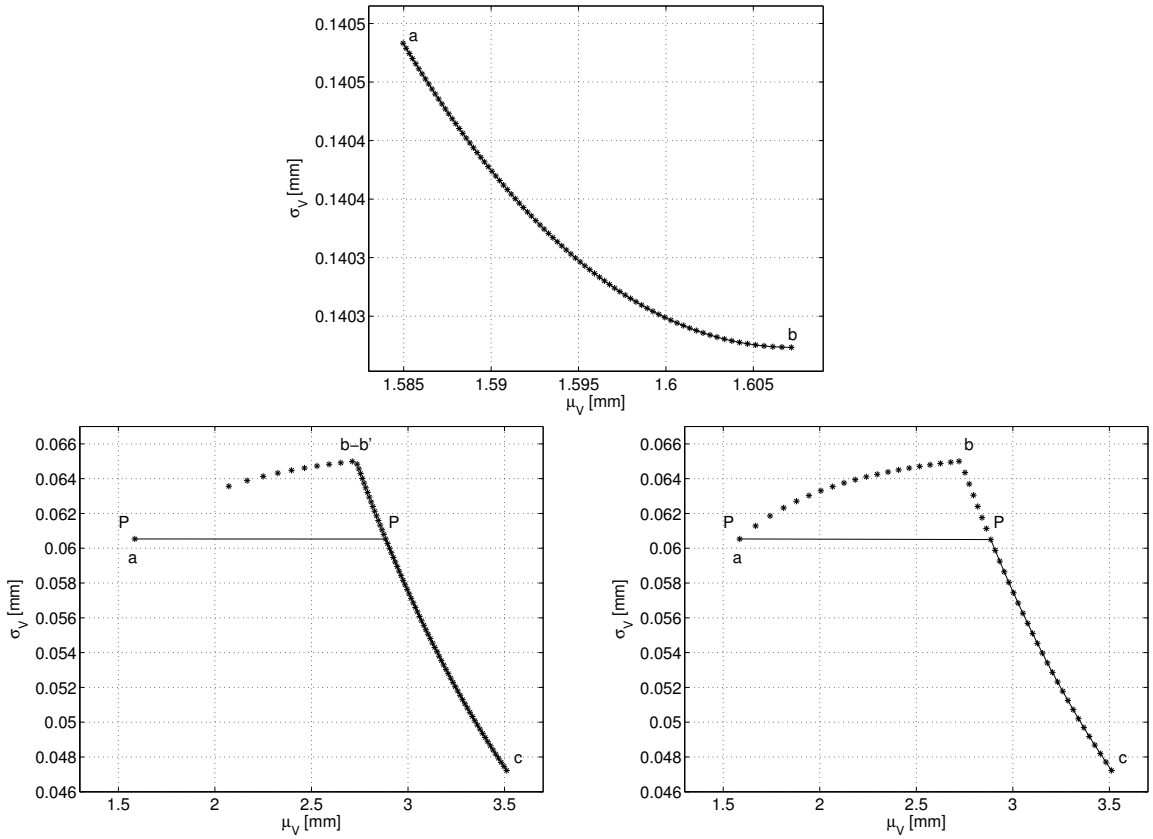

Figure 10: Pareto front of the two-bar truss for the frequency band $(100, 300)$ Hz (up) and $(600, 800)$ Hz (down)

NBI method in conjunction with the penalty method are applied successfully to transform the two multi-objective problems of interest into unconstrained single-objective problems, while the RFNM algorithm is proposed to solve them. The RFNM algorithm is a new hybridization approach, based on the combination of a modified Pincus representation formula and the Simplex (Nelder-Mead) algorithm. The main advantage of this hybridization is the high reliability and stability of the algorithm, even when the penalty method is applied.

The results showed that RFNM is able to locate the global optimum with accuracy and it is simple to be applied to general design problems although it is slightly expensive. They also shows that the NBI method can produce an even spread set of Pareto points for an adequate choice of the normal to the convex hull of the minima of the objective functions. While the first problem is somewhat standard and the resulting Pareto curve presents no novelty, the second problem is more interesting and the position of the optimal point for the variance changes with the frequency band chosen for the load. Indeed, this simple two bar truss problem has a remarkable shape for the Pareto front for the frequency band $(600, 800)$ Hz since it is discontinuous, due to multiple minima involved within this situation and the presence of an anti-resonant frequency.

Thus, it is shown through this example that some difficult situations can occur for designing the mechanical systems when considering their dynamic responses due to random loads, even for a simple case as of a linear systems subject to Gaussian load. But the strategy proposed here has shown its ability to give valuable results and it can help designers to choose for the best compromise between the mean and the standard deviation for this kind of problems.

REFERENCES

Avriel M. *Nonlinear Programming: Analysis and Methods*. Prentice-Hall, Englewood Cliffs, NJ, 1976.

Bez E., Souza de Cursi J., and M.B. G. Um procedimento numerico para a otimizatio global baseado em uma representatio da solutio. *Tema - Tend. Mat. Apl. Comput.*, 5(2):185–194, 2004.

Charnes A. and Wolfe M. Extended pincus theorems and convergence of simulated annealing. *Int. J. Systems Sci.*, 20(8):1521–1533, 1989.

Chelouah R. and Siarry P. A hybrid method combining continuous tabu search and nelder-mead simplex algorithms for the global optimization of multiminima functions. *Eur. J. Operat. Res.*, 161, 2005.

Collette Y. and P. S. *Multi-objective optimization: principles and case studies*. Springer, 2003.

Das I. and Dennis J. Normal-boundary intersection: a new method for generating pareto optimal point in nonlinear multicriteria optimization problems. *SIAM Journal on Optimization*, 8(3):631–657, 1998.

Davidor Y. A viewpoint on ga-hardness. In *Proceedings of the First Workshop on Foundations of Genetic Algorithms*, pages 23–35. 1990.

Falk J. Condition for global optimization in nonlinear programming. *Operation Research*, 21:337–340, 1973.

Fan S. and Zahara E. Hybrid simplex search and particle swarm optimization for unconstrained optimization problems. *European Journal of Operation Research*, 181:527–548, 2007.

Floudas, Christodoulos, Pardalos, and Panos. *Encyclopedia of Optimization*. Springer, 2009.

Géradin M. and Rixen D. *Théorie des Vibrations - Applications à la Dynamique des Structures*. Ed. Masson, 1996.

Gillespie T. *Fundamentals of vehicle dynamics*. Society of Automotive Engineers, 1992.

Ivorra B., Mohammadi B., Ramos A., and Redont P. Optimizing initial guesses to improve global minimization. *Journal Of Global Optimization*, 2011.

Lee K. and El-Sharkawi M. *Modern Heuristic Optimization Techniques: Theory and Applications to Power Systems*. IEE, New York, 2008.

Lin Y. *Probabilistic theory of structural dynamics*. McGraw-Hill, Inc., N.Y., 1967.

Luenberger D. *Introduction to Linear and Nonlinear Programming*. Stanford University, 1973.

Nelder J. and Mead R. A simplex method for function minimization. *Computer Journal*, 7:308–313, 1965.

Pincus M. A closed formula solution of certain programming problems. *Operations Research*, 16(3):690–694, 1968.

Pincus M. A monte carlo method for the approximate solution of certain types of constrained optimization problems. *Operation Research*, 18:1225, 1970.

Souza de Cursi J. *Representation of Solutions in Variational Calculus*. E. Tarocco; E. A. de Souza Neto; A. A. Novotny , (Org.). Variational Formulations in Mechanics: Theory and Applications. Barcelona , (CIMNE), 2007.

Souza de Cursi J., Bez E., and Goncalves M. A procedure of global optimization and its application to estimate parameters in interaction spatial models. In *EngOpt 2008*. 2008.

Wijker J. *Random Vibrations in Spacecraft Structures Design*. Springer Verlag, 2009.